Magnetic Resonance Imaging 99 (2023) 20–25

Contents lists available at ScienceDirect

Magnetic Resonance Imaging

journal homepage: www.elsevier.com/locate/mri

4D segmentation of the thoracic aorta from 4D flow MRI using deep learning

Diana M. Marin-Castrillon [a], Alain Lalande [a,b], Sarah Leclerc [a], Khalid Ambarki [c], Marie-Catherine Morgant [a,d], Alexandre Cochet [a,b], Siyu Lin [a], Olivier Bouchot [a,d], Arnaud Boucher [a], Benoit Presles [a,*]

[a] Imaging and Artificial Vision Laboratory, EA 7535, University of Burgundy, Dijon 21000, France
[b] Medical Imaging Department, University Hospital of Dijon, Dijon 21000, France
[c] Siemens Healthcare SAS, Saint-Denis 93200, France
[d] Department of cardiovascular and thoracic surgery, University Hospital of Dijon, Dijon 21000, France

ARTICLE INFO

Keywords:
4D flow MRI
Deep learning
Segmentation
Thoracic aortic aneurysm

ABSTRACT

Background: 4D flow MRI allows the analysis of hemodynamic changes in the aorta caused by pathologies such as thoracic aortic aneurysms (TAA). For personalized management of TAA, new biomarkers are required to analyze the effect of fluid structure iteration which can be obtained from 4D flow MRI. However, the generation of these biomarkers requires prior 4D segmentation of the aorta.
Objective: To develop an automatic deep learning model to segment the aorta in 4D from 4D flow MRI.
Methods: Segmentation is addressed with a U-Net based segmentation model that treats each 4D flow MRI frame as an independent sample. Performance is measured with respect to Dice score (DS) and Hausdorff distance (HD). In addition, the maximum and minimum surface areas at the level of the ascending aorta are measured and compared with those obtained from cine-MRI.
Results: The segmentation performance was 0.90 ± 0.02 for the DS and the mean HD was 9.58 ± 4.36 mm. A correlation coefficient of $r = 0.85$ was obtained for the maximum surface and $r = 0.86$ for the minimum surface between the 4D flow MRI and cine-MRI.
Conclusion: The proposed automatic approach of 4D aortic segmentation from 4D flow MRI seems to be accurate enough to contribute to the wider use of this imaging technique in the analysis of pathologies such as TAA.

1. Introduction

An aortic aneurysm is an increase in diameter greater than or equal to 50% of its expected size [1]. As a consequence of this pathology, the aortic wall can rupture or dissect, causing lethal consequences. The overall incidence per year of thoracic aortic aneurysms (TAAs) is 5 to 10 per 100,000 people, becoming the 19th leading cause of death overall [2]. In clinical practice, the decision to intervene surgically on an aneurysm is mainly taken considering its diameter and growth rate. However, it has been observed that rupture and dissection can occur in aneurysms smaller than the sizes indicated in the guidelines [3,4]. Therefore, the generation of new biomarkers (including aorta shape, movement and constrain flow) that allow a personalized treatment of TAA is essential. In this context, 4D flow MRI is a cornerstone for assessing these parameters and opens the door to a new way of analyzing by considering the local and global hemodynamic characteristics and particularly the changes produced by cardiovascular pathologies such as TAA.

Despite the potential of 4D flow MRI for a widespread use in clinical practice for flow analysis and biomarker computation, it is necessary to first overcome some challenges such as automatic segmentation of the aortic wall. In the literature, in most studies, only 3D segmentation is proposed on 3D images generated from 4D flow MRI. The main objective of generating 3D images is to enhance the contrast between the aorta and the background. Kohler et al. [5] generated a maximum intensity projection image (tMIP) using the time steps of the magnitude image. Then, they ran a graph cut-based algorithm manually initialized by a user. Similarly, other studies have applied pre-processing techniques to create a 3D phase contrast magnetic resonance angiography (PCMRA) image from 4D flow MRI [6–8]. The drawback with PCMRA generation

* Corresponding author.
E-mail address: benoit.presles@u-bourgogne.fr (B. Presles).

https://doi.org/10.1016/j.mri.2022.12.021
Received 29 August 2022; Received in revised form 24 December 2022; Accepted 31 December 2022
Available online 5 January 2023

is that the temporal information is lost, which leads to a bias in the position of the aorta. Using PCMRA, active surface [6], or 3D neural networks [7,8] based segmentation algorithms have been implemented. Although these methods have shown high performance on PCMRA images, generating the segmentation for the whole cardiac cycle with comparable results is still an open problem.

To address a 4D segmentation, Bustamante et al. [9] proposed the generation of a 4D PCMRA image by applying intra-patient registration to a tMIP image generated from 3D PCMRAs calculated independently for each time step. Then, they automatically segmented the heart and large thoracic vessels with a multi-atlas-based algorithm. A limitation of this method is that it relies on the quality of the intra-patient registration to preserve the aorta position during the cardiac cycle. In addition, the computational time required for the segmentation of a new patient is considerably high compared to deep learning-based methods. Recently, the same team proposed a 4D segmentation of these organs using a 3D deep learning model [10] trained directly on the magnitude images. With this pipeline, promising segmentation results were obtained on their database. However, the patient population used to evaluate the approach presented heart pathologies or mitral valve regurgitation but no aneurysm at the level of the thoracic aorta (TAo). Moreover, the ground truth used in the training of the deep learning model was automatically generated with a multi-atlas-based method and then maybe is questionable.

The main objective of this work is to design an automatic method for the segmentation of the aorta from 4D flow MRI on patients with TAA. Therefore, we proposed a method similar to that of Bustamante et al. [10] to segment the aorta in 4D from 4D flow MRI using a specific database of patients with TAA. We evaluated the ability of such a method to adapt to the different shapes of the aorta during the cardiac cycle. For this purpose, the maximum and minimum surface areas at the level of the ascending aorta acquired from 4D flow MRI were compared with those calculated from cine-MRI, the image conventionally used for this type of metric.

2. Data

2.1. Study population

In this study were included 36 subjects that consented to participate to the project 2018-A02010–55, approved by the national ethic committee (”Comité de Protection des Personnes”). The study has been registered on ClinicalTrials.gov with the number NCT03817008. All 36 patients had TAA at the level of the ascending aorta. Ten patients in the cohort were female and 26 were male. Half of the men and half of the women had tricuspid aortic valve, the others had bicuspid aortic valve. Bicuspid aortic valve is an anomaly that affects 2% of the population and can cause the formation of aortic aneurysms. The average age of the patients was 60 years.

2.2. MRI examinations

All patients underwent 4D flow MRI acquisition on a 3 T Siemens magnet (Skyra, Siemens Healthineers, Erlangen, Germany) after the injection of a Gadolinium-based contrast agent. The 4D flow MRI was retrospective electrocardiogram (ECG) gated during free breathing. The diaphragm movement was managed using an echo navigator. In our 4D flow MRI protocol, 25 time steps of the cardiac cycle were acquired with a time resolution of 24 to 52 ms according to the patient's heart rate. The spatial resolution was set at $2 \times 2 \times 2\ mm^3$ and the velocity encoding (Venc) in the range of 200 to 800 cm/s. Echo and repetition times were set between 2.1 and 2.3 and 38.5–40 ms, respectively. The acquisition took 10 to 15 min according to the patient. During the image reconstruction, non-uniform intensity correction and a 2D distortion correction were performed.

The FLASH sequence (Fast Low Angle SHot) was used for the acquisition of the cine-MRI. The acquisition was performed during breath-hold in a plane perpendicular to the aorta at the level of the pulmonary trunk. From this sequence, 35 phases of the cardiac cycle were acquired with a temporal resolution between 20 and 34 ms. The spatial resolution was set between 1.25×1.25 and $1.9 \times 1.9\ mm^2$. The echo and repetition time were equal to.

3. 42 and 34 ms, respectively

3.1. Ground truth generation

For the training and performance evaluation of the deep learning-based segmentation algorithm, an image analyst generated 4D manual segmentations of the aorta (five different time points for each patient). Segmentations were generated using the ITK-SNAP software [11]. ITK-SNAP software allows segmentation in sagittal, axial, or coronal orientations and has as reference the three views simultaneously displayed during the drawing. Then, the 3D segmentation for each time frame was done considering these three planes. In the segmentation generated with ITK-SNAP, the aortic lumen is labeled and not only the border. To select the frames to be segmented, we calculated the average velocity at each time step on an axial 2D plane at the level of the ascending aorta (AAo). This plane is extracted from the 4D flow MRI. Since the acquisition begins at the end of diastole, the first image was segmented for all patients. The frame corresponding to the maximum average velocity computed was also segmented as systolic phase. To reduce the time of the manual segmentation of the remaining three frames, the diastolic segmentation was taken as the starting segmentation and corrected to fit the aorta of the frames numbered 15, 20, and 25. Because of the low quality of the magnitude images, it is impossible to define accurately the border of the brachiocephalic artery, left common carotid artery, and left subclavian artery. For this reason, these arteries were not included in the segmentation. Moreover, since the drawing of the aortic valve sinuses from 4D flow MRI is very difficult and subject to inter observer-variability, a flat segmentation was performed at the level of the aortic sinuses. All the manual segmentations were reviewed by a clinical expert.

4. Method

4.1. Network architecture

The neural network used is based on 3D U-Net (Fig. 1). It is composed of one encoder and one decoder path with skip connections [12]. Its architecture is four levels deep, meaning there are four spatial sampling operations. The encoder path is composed of convolution layers with a kernel size of $3 \times 3 \times 3$ pixels followed with batch normalization and rectified linear unit (ReLu) activation layers. Max pooling with a stride of two is used to move to the next level. To perform the expansion in the decoder path, an up-sampling operation is performed. Finally, the probability of a pixel belonging to the aorta or background is obtained with the softmax function. The images were cropped or padded considering the mean size on the database for the x and y axes. For the z axis, the maximum size was set. Thus, a size of $146 \times 176 \times 44$ voxels were obtained for all the images. Then, to speed up the training, the spacing was transformed to $4 \times 4 \times 4\ mm^3$, so the size of the input images to the network was $73 \times 88 \times 22$ voxels.

4.2. Training of the network

Before training the model, the magnitude images were normalized independently between 0 and 1. The model was implemented in PyTorch [13] and was trained for 500 epochs with a batch size equal to four. The Adam optimizer was used with the Dice loss. The latter was computed by excluding the background to only focus on the aorta. The learning rate was initialized at 0.01 and reduced by a factor equal to ten

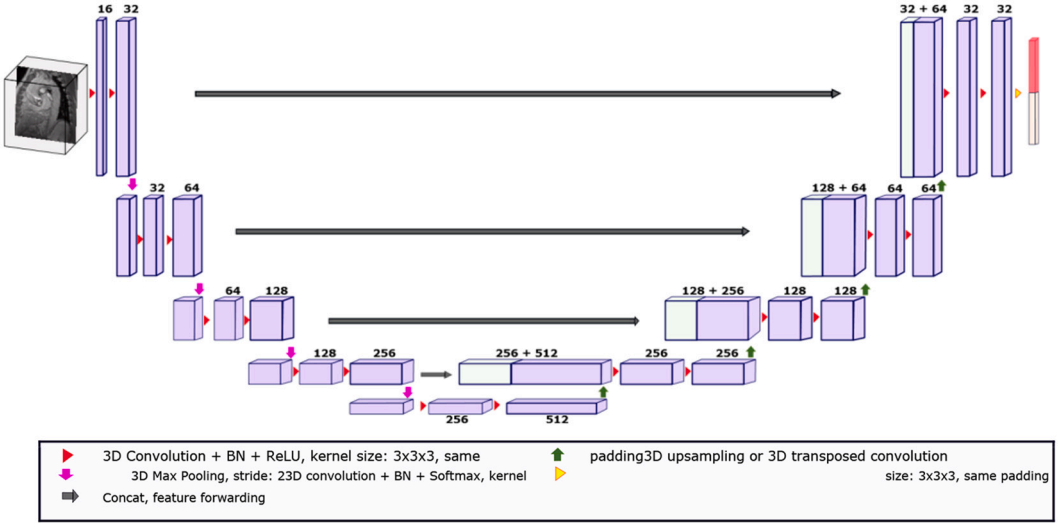

Fig. 1. 3D U-Net architecture used. The numbers above the blocks indicate the number of feature maps.

once validation loss stopped improving. As our dataset is small, the 3D U-Net was trained with a leave-one-patient-out cross validation strategy. Leave-one-patient-out cross-validation strategy is a specific application of k-fold cross validation, where k is equal to the number of patients. Thus, for each patient selected as a test set, 35 patients (35 patients × 5 frames = 175 frames) were used for training. The five manually segmented frames of the test patient were used for testing. There is no validation set. It should be noted that this 3D U-Net-based 4D segmentation approach treats each frame as an independent sample. As post-processing, the largest connected component in the segmentation was identified and selected. Later, segmentation smoothing was performed with morphological opening filter.

4.3. Performance evaluation

To perform a global and a local analysis of the segmentation results, the aorta was divided into AAo including the arch (AAo + Arch) and the descending thoracic aorta (TDAo).

The overlap between the manual (A) and the automatic (B) segmentations was measured using the DSC to obtain information on the global segmentation performance (Eq. (1)). This index is bounded between zero and one, one represents a perfect overlap, and zero means no overlap

$$DSC(A,B) = 2\frac{A \cap B}{|A| + |B|} \tag{1}$$

To analyze the error at the level of the contour and to detect outliers, the Hausdorff distance (HD) was calculated. In the case of two finite point sets $A = [a_1, \ldots, a_p]$ and $B = [b_1, \ldots, b_p]$, the Hausdorff is defined as follows:

$$HD(A,B) = max(h(A,B), h(B,A)) \tag{2}$$

where

$$h(A,B) = \underset{a \in A}{max} \underset{b \in B}{min} \|a - b\| \tag{3}$$

$h(A,B)$ is the one-sided HD and $\|\cdot\|$ is a measure of distance as the Euclidean norm. Thus, the function $h(A,B)$ identifies the point a farthest from any point of B. Then, it measures the distance from a to its nearest neighbor in B [14].

The minimum and maximum surfaces over the cardiac cycle were computed in a 2D + time axial plane extracted from the 4D segmentation of the aorta, taking as reference the pulmonary trunk. To take into account for the soft temporal displacement of the aorta from diastole to systole we lastly apply a morphological opening filter on the extracted 2D + time axial plane using a ball structuring element of radius 2 mm.

For comparison, the minimum and maximum reference surfaces were computed from the 2D + time cine-MRI in the same localization with an automatic algorithm based on the method described by Miteran et al. [15].

Pearson correlation of the minimum and maximum surface values obtained from 4D flow MRI and cine-MRI were calculated in order to measure the association between two sets of area values acquired with the two different approaches. Moreover, in order to determine if there is a statistical difference between the mean of these two sets of data, a paired sample *t*-test was performed after testing the normality of the samples with Shapiro-Wilk test. The paired sample t-test is complementary. For static tests, a confidence interval of 99% is considered. Finally, the maximum and minimum surface areas were compared using Bland-Altman analysis [16].

As our method is fully automatic and requires no interaction with experts during the process, the study of its reproducibility is not necessary.

5. Results

The average global segmentation performance over the 180 frames was 0.90 ± 0.02 and 9.58 ± 4.36 mm for DSC and HD, respectively. Locally, similar performance was obtained for the AAo + Arch and TDAo (Table 1). Fig. 2 shows the patients with the best and worst segmentation results concerning the global 3D DSC and global 3D HD. The lowest segmentation performance concerning HD occurred in a patient with signal degradation at the distal TDAo level during acquisition. However, this is an outlier, and the rest of the patients obtained a lower one-sided HD, as shown in Fig. 3.

The maximum and minimum surfaces areas obtained from 4D flow MRI and cine-MRI showed a high correlation with a correlation coefficient r of 0.85, and 0.86 respectively. The regression plots are presented in Fig. 4 and Fig. 5.

Table 1
Average performance of 3D U-net in 4D aortic segmentation from 4D flow MRI.

AAo + Arch		TDAo		GLOBAL	
DSC	HD (mm)	DSC	HD (mm)	DSC	HD (mm)
0.90 ± 0.02	8.75 ± 3.00	0.89 ± 0.02	7.19 ± 6.03	0.90 ± 0.02	9.58 ± 4.36

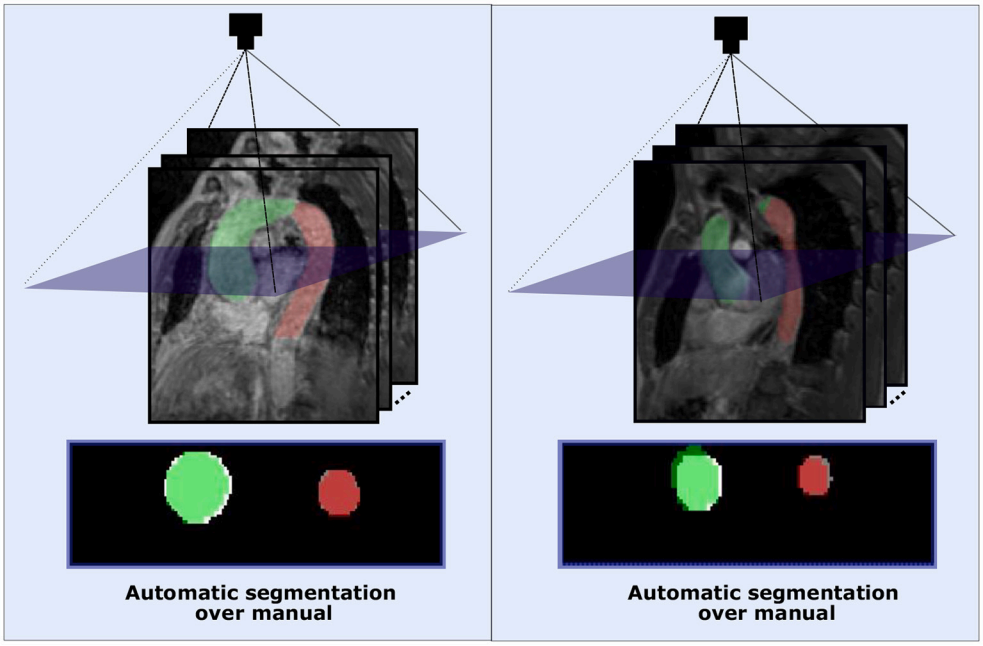

Fig. 2. Slices for patients with the highest (left image) and lowest (right image) performance concerning the 3D DSC and the 3D HD measured. On the bottom, the automatic segmentation (green and red colors) is superimposed on the manual segmentation (in white). The 2D plane displayed represents the one extracted at the level of the pulmonary trunk for the maximum and minimum surface area evaluation. (For interpretation of the references to colour in this figure legend, the reader is referred to the web version of this article.)

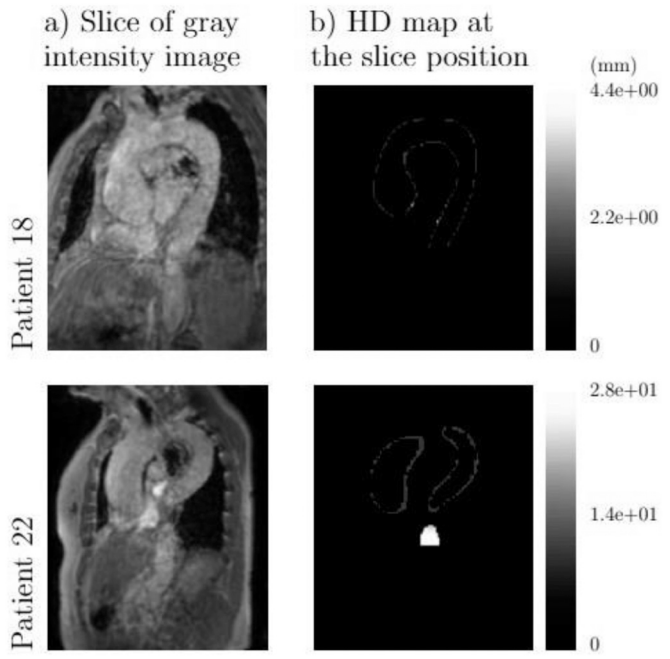

Fig. 3. Patients with the lowest and highest Hausdorff distance a) Slice of the gray intensity image. b) One-sided HD map computed between the manual and automatic segmentation for the slice of the gray image.

The paired sampled *t*-test showed that there is no significant statistical difference between the minimum surfaces calculated from 4D flow MRI and cine-MRI. Here the null hypothesis of zero mean was approved with a p-value = 0.15 [CI: −36.70123.62]. For the paired t-test carried out with the maximum surfaces, the *p*-value obtained was right on the acceptance limit of the null hypothesis of no significant difference, p-value = 0.0097 [CI: −163.82 -0.37]. The Bland-Altman analysis between the maximum surface measured with cine-MRI and 4D flow MRI showed an average difference of $-82.12 \pm 174.63\ mm^2$. For the minimum surface, the average difference was $43.56 \pm 171.25\ mm^2$ (Fig. 6).

The training of the U-Net model took about one hour for each

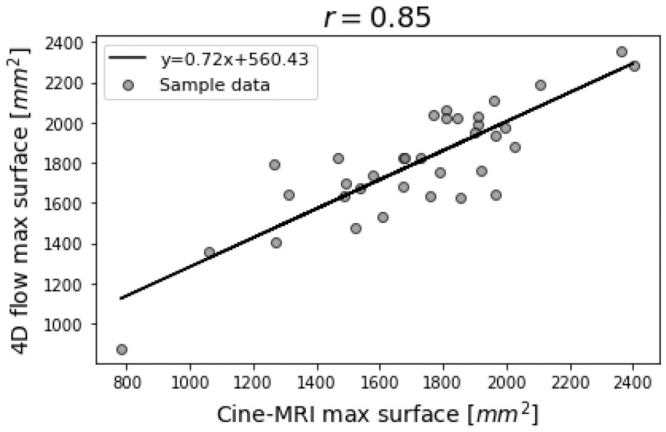

Fig. 4. Correlation of the maximum surface calculated from 4D flow MRI and from cine-MRI. *r* is the correlation coefficient obtained between the maximum surfaces.

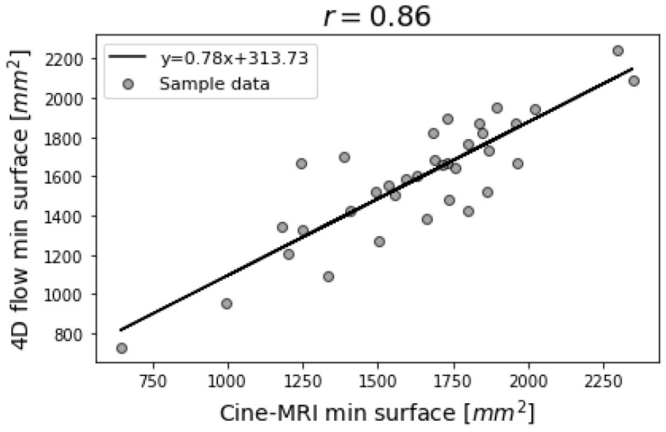

Fig. 5. Correlation of the minimum surface calculated from 4D flow MRI and from cine-MRI. *r* is the correlation coefficient obtained between the minimum surfaces.

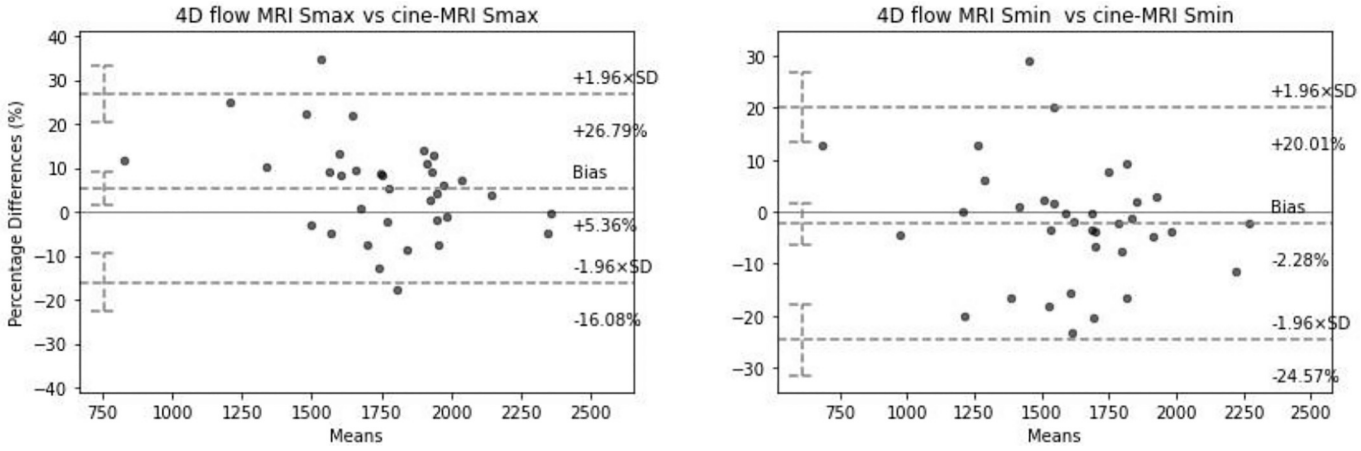

Fig. 6. Bland-Altman plots of the maximum and minimum surface areas obtained at the level of the ascending aorta during the cardiac cycle.

patient. The prediction of the whole cardiac cycle segmentation took only about 10 s for each patient on a laptop workstation Dell Precision 7540 with CPU Intel Core i7-9850H at 2.60GHz processor. In comparison, manual segmentation from scratch of a single frame takes about 3 h (75 h for all time frame per patient.

6. Discussion

In this study, we segmented the thoracic aorta over the cardiac cycle in patients with aneurysms by using a method based on the one proposed by Bustamante et al. [10]. Then, for each time point of the cardiac cycle, the aorta was segmented using a 3D U-Net model on the magnitude image of the 4D flow MRI. By doing so, we avoid the biases inherent in the generation of new images from 4D flow MRI. Compared to the work of the Bustamante et al. [10], dilated aorta segmentation is more challenging than segmentation on healthy patients due to image degradation. The reduction in quality is generally caused by cardiac arrhythmia and double systole peaks in the ECG that affect the acquisition, in particular when it is retrospective gating. Thus, the aim of evaluating this approach was to contribute to the standardization of automatic 4D aortic segmentation techniques from 4D flow MRI by presenting the segmentation results in a dataset of patients with TAA. Moreover, it is important to note that the way we have constructed our ground truth differs from theirs. In their case, an inter-patient multi-atlas-based segmentation method was used to segment the end of systole and of.

diastole before applying an intra-patient registration algorithm to segment the other time frames. The quality of the ground truths generated with this method is related to the parameters chosen by the user for the registration, which are generally not adequate for all patients. Segmentation may even fail for some patients. It is the case for about 4% of patients in Bustamante et al.'s database. In our case, for all patients, we segmented manually five time frames and they were all reviewed by an expert. With manually generated ground truths, the model's performance is directly compared to that of an expert, avoiding the propagation of errors from an automatic method to the evaluated one.

On our dataset, the evaluated method gives promising results. The average DSC value computed on 180 volumes was 0.9 ± 0.02. The lowest performance was presented in a frame corresponding to diastole. The low performance was directly related to signal loss during acquisition in the distal TDAo. However, in this frame, the degradation did not affect the AAo + Arch or the proximal TDAo, and a low HD were obtained in these regions (Fig. 3). In general, discrepancies between manual and automatic segmentations occurred at the level of the aortic valve or at the level of the aortic arch. In these regions, the differences were generally around 5 voxels (for 87% of the samples), relatively low considering particularly the challenges in drawing.

the valve both manually and automatically. Specifically, the discrepancies at the level of the aortic valve might be due to the manual segmentation which is flat at this location. At the level of the aortic arch, the automatic segmentation sometimes includes voxels belonging to the brachiocephalic arteries. These voxels are considered as segmentation errors since they are not present in the manual segmentation. Our results are comparable to those obtained by Bustamante et al. [10] (average $DSC = 0.93 \pm 0.03$) with a database without TAA. Concerning 3D PCMRA aortic segmentation methods, Berhane et al. [7] achieved a slightly better performance than ours for DSC, obtaining a median of 0.95. Although segmentation from PCMRA is facilitated by contrast enhancement between the aorta and the background, the position of the aorta during the cardiac cycle is questionable. In addition, generating this image can result in PCMRAs with degradation of aorta shape, mainly at the level of the aortic valve.

For further analysis of the behavior of the segmentation method in the temporal dimension, its ability to adapt to the different shapes of the aorta during the cardiac cycle was evaluated. For this purpose, the maximum and minimum surfaces calculated in a 2D + time image extracted from the 4D segmentation was compared with the ones extracted from 2D + time cine-MRI. The maximum and minimum surfaces are relevant as metrics because they represent the dynamic expansion of the aorta exerted to soften the pressure on the wall caused by the variable blood flow during the cardiac cycle. In the presence of aortic pathologies, the elasticity of the aorta could be affected [17], and these measurements could provide information about it. One might also evaluate the efficiency of our method by comparing the volume of the thoracic aorta obtained with our automatic method and by manual drawing, but it is difficult to define accurately and in a reproducible way the planes corresponding to the beginning and the end of these volumes. Thus, we prefer to consider the surfaces obtained at a well-defined anatomically plane. Both 2D + time images were located perpendicular to the axis of the ascending aorta and taking as reference the pulmonary trunk. Then, the maximum and minimum surfaces were calculated at the level of the AAo. For both surfaces, a strong correlation (correlation coefficients >0.85) with no statistically significant differences between the two methods was obtained. It should be noted that the highest difference between the two methods is obtained with the maximum surface area. In the *t*-test with maximum surfaces, the *p*-value at the limit of acceptance of the null hypothesis reflects this as well (cf. Fig. 6). This may be related to the different physiological conditions during the acquisition and the kind of imaging protocols for cine-MRI and 4D flow MRI. In particular, a force is exerted on the thorax by holding the breath during the cine-MRI acquisition as the 4D flow MRI acquisition is in free breathing. Moreover, the temporal resolution of this sequence is better than 4D flow MRI.

The segmentation performance and the maximum and minimum

surface analysis showed that it is possible to obtain reliable TAo segmentations with the proposed method. In particular, the surface analysis results suggest that it is possible to calculate from 4D flow MRI metrics usually calculated in 2D + time sequences such as peak pressure or maximum diameter. Moreover, it also encourages the exploration of biomarkers correlated with aortic dilatation such as wall shear stress [18]. Indeed, in most of the studies, this parameter has been calculated usually assuming a static aorta. This assumption produces bias in the biomarker computation [19,20].

In the future, the database should be enlarged to include more anatomical differences between patients during the training and reduce the possible variance of the segmentation of new data. When the database is sufficiently developed, it will be interesting to evaluate the possibility of a learning method integrating the temporal dimension to compare the results obtained with a succession of 3D segmentations, as presented in this study, to those obtained with a 4D approach. Moreover, the use of images acquired from a single MRI scan is a limitation. For a broader evaluation, a multi-center study should be considered.

7. Conclusion

The method evaluated in this paper for 4D segmentation of dilated aorta from 4D flow MRI magnitude images showed results comparable to those obtained in recent works for 4D segmentation of subjects without this pathology. Results shows that the 3D model adapts to the various shapes of the aorta during the cardiac cycle. Thus, the proposed approach of 4D aortic segmentation from 4D flow MRI could contribute to the expanded use of 4D flow MRI in the analysis of pathologies such as TAA. The results encourage further exploration of biomarkers correlated with aortic dilatation, such as wall share stress that, due to the challenge in 4D segmentation, have currently been evaluated assuming a static aorta.

References

[1] Saliba E, Sia Y, Dore A, El Hamamsy I. The ascending aortic aneurysm: when to intervene? IJC Heart Vasc 2015;6:91–100.

[2] Pinard A, Jones GT, Milewicz DM. Genetics of thoracic and abdominal aortic diseases: aneurysms, dissections, and ruptures. Circ Res 2019;124(4):588–606.

[3] Pape L, Tsai T, Isselbacher E, Oh J, O'gara P, Evangelista A, et al. International registry of acute aortic dissection IRAD investigators: aortic diameter > or= 5.5 cm is not a good predictor of type a aortic dissection: observations from the international registry of acute aortic dissection IRAD. Circulation 2007;116:1120–7.

[4] Adamo L, Braverman AC. Surgical threshold for bicuspid aortic valve aneurysm: a case for individual decision-making. Heart 2015;101(17):1361–7.

[5] Kohler B, Preim U, Grothoff M, Gutberlet M, Fischbach K, Preim B. Guided analysis of cardiac 4d pc-mri blood flow data. Eurographics 2015;2015:2–5.

[6] van Pelt R, Nguyen H, ter Haar Romeny B, Vilanova A. Automated segmentation of blood-flow regions in large thoracic arteries using 3dcine pc-mri measurements. Int J Comput Assist Radiol Surg 2012;7(2):217–24.

[7] Berhane H, Scott M, Elbaz M, Jarvis K, McCarthy P, Carr J, et al. Fully automated 3d aortic segmentation of 4d flow mri for hemodynamic analysis using deep learning. Magn Reson Med 2020;84(4):2204–18.

[8] Fujiwara T, Berhane H, Scott MB, Englund EK, Schafer M, Fonseca B, et al. Segmentation of the aorta and pulmonary arteries based on 4d flow mri in the pediatric setting using fully automated multi-site, multivendor, and multi-label dense u-net. J Magn Reson Imaging 2022;55(6):1666–80.

[9] Bustamante M, Gupta V, Forsberg D, Carlhall C-J, Engvall J, Ebbers T. Automated multi-atlas segmentation of cardiac 4d flow mri. Med Image Anal 2018;49:128–40.

[10] Bustamante M, Viola F, Engvall J, Carlhall C-J, Ebbers T. Automatic time-resolved cardiovascular segmentation of 4d flow mri using deep learning. J Magn Reson Imaging 2022;57:191–203.

[11] Yushkevich PA, Piven J, Hazlett HC, Smith RG, Ho S, Gee JC, et al. User-guided 3d active contour segmentation of anatomical structures: significantly improved efficiency and reliability. Neuroimage 2006;31(3):1116–28.

[12] Janssens R, Zeng G, Zheng G. Fully automatic segmentation of lumbar vertebrae from ct images using cascaded 3d fully convolutional networks. In: 2018 IEEE 15th International Symposium on Biomedical Imaging (ISBI 2018). IEEE; 2018. p. 893–7.

[13] Paszke A, Gross S, Chintala S, Chanan G, Yang E, DeVito Z, et al. Automatic differentiation in pytorch. 2017.

[14] Huttenlocher DP, Klanderman GA, Rucklidge WJ. Comparing images using the hausdorff distance. IEEE Trans Pattern Anal Mach Intell 1993;15(9):850–63.

[15] Mit'eran J, Bouchot O, Cochet A, Lalande A. Automatic determination of aortic compliance based on mri and adapted curvilinear detector. Biomed Signal Process Control 2018;40:295–311.

[16] Giavarina D. Understanding bland altman analysis. Biochem Med 2015;25(2):141–51.

[17] Harky A, Sokal PA, Hasan K, Papaleontiou A. The aortic pathologies: how far we understand it and its implications on thoracic aortic surgery. Braz J Cardiovas Surg 2021;36:535–49.

[18] Burris NS, Sigovan M, Knauer HA, Tseng EE, Saloner D, Hope MD. Systolic flow displacement correlates with future ascending aortic growth in patients with bicuspid aortic valves undergoing magnetic resonance surveillance. Invest Radiol 2014;49(10):635–9.

[19] Perinajova R, Juffermans JF, Westenberg JJ, van der Palen RL, van den Boogaard PJ, Lamb HJ, et al. Geometrically induced wall shear stress variability in cfd-mri coupled simulations of blood flow in the thoracic aortas. Comput Biol Med 2021;133:104385.

[20] Soulat G, Scott MB, Allen BD, Avery R, Bonow RO, Malaisrie SC, et al. Association of regional wall shear stress and progressive ascending aorta dilation in bicuspid aortic valve. Cardiovas Imaging 2022;15(1):33–42.